Visible radiophotoluminescence of colour centres in lithium fluoride: from lasers to versatile radiation sensors

Visible radiophotoluminescence of colour centres in lithium fluoride: from lasers to versatile radiation sensors

R.M. Montereali[1], F. Bonfigli[1], E. Nichelatti[2], V. Nigro[1], M. Piccinini[1], M.A. Vincenti[1]
[1]ENEA C.R. Frascati, Fusion and Technologies for Nuclear Safety and Security Department, Via E. Fermi 45, 00044 Frascati (Rome), Italy
[2]ENEA C.R. Casaccia, Fusion and Technologies for Nuclear Safety and Security Department, Via Anguillarese 301, 00123 S. Maria di Galeria (Rome), Italy
e-mail: rosa.montereali@enea.it

Abstract. The peculiar photoluminescence characteristics of radiation-induced colour centres in lithium fluoride (LiF), well known for applications in optically-pumped tuneable lasers and broad-band miniaturised light-emitting photonic devices operating at room-temperature, are under exploitation in passive imaging detectors and dosimeters based on visible radiophotoluminescence in LiF crystals and polycrystalline thin films. Their high intrinsic spatial resolution, wide dynamic range and large field of view, combined with easy handling, ambient-light operation and no development need, allow to successfully extend their use from X-ray imaging to proton-beam advanced diagnostics and dosimetry, even at those low dose values that are typical of hadrontherapy. After exposure, the latent images stored in LiF as local formations of F_2 and F_3^+ aggregate defects are read with an optical fluorescence microscope under illumination in the blue spectral range. Their visible emission intensity was found to be linearly proportional to the dose over at least three orders of magnitude, so that bi-dimensional LiF solid-state dosimeters based on spectrally-integrated radiophotoluminescence reading can be envisaged. Taking advantage of the low thickness of LiF thin films, transversal proton beam dose mapping was demonstrated at low proton energies, even at high doses. Recent results and advances concerning LiF crystals and polycrystalline thin film characterisation in the linearity range are presented and discussed with the aim of highlighting challenges related to increasing the LiF film detector radiation sensitivity to both particles (protons) and photons (X-rays), although therapeutic dose values typical of clinical radiotherapy are still a big challenge.

1. Introduction

Luminescence properties of point defects in insulating materials are successfully used for solid-state light sources and radiation sensors. The peculiar radiophotoluminescence (RPL) characteristics of aggregate colour centres (CCs) in lithium fluoride (LiF), well known for applications in optically-pumped tuneable lasers [1] and broad-band miniaturised light-emitting photonic devices [2] operating at room-temperature (RT), are under exploitation in solid-state passive radiation imaging detectors [3-7] and dosimeters [8-11] based on the visible PL of radiation-induced F_2 and F_3^+ CCs in LiF crystals [5,8,11] and thin films [3,4,6,7,9,10].

The photoluminescent LiF-based radiation detectors have interesting characteristics, like very high intrinsic spatial resolution, related to the nanometric dimensions of electronic defects [12], wide dynamic range and large field of view, limited only by technologies of growth processes of LiF crystals and thin films. Moreover, these solid state radiation detectors are easy to handle, being insensitive to ambient light, thanks to the stability of CCs at RT in LiF, and no development process is needed.

These peculiarities, combined with the ionising radiation sensitivity of LiF, allow to successfully use LiF-based radiation detectors for extreme ultraviolet, soft and hard X-ray imaging experiments [3-7] and, more recently, to extend their use to proton beam advanced diagnostics [9,10] and X-ray clinical dosimetry [8], even at those low dose values that are typical of hadrontherapy [11]. It should be noticed that a reusable tissue-equivalent solid-state dosimeter with linear dose response, high

spatial resolution and excellent radiation hardness is needed for radiation therapy dosimetry, but is not available yet.

The laser-active F_2 and F_3^+ centres, consisting of two electrons bound to two and three adjacent anion vacancies, respectively, possess almost overlapping absorption bands peaked at ~450 nm, which together form what is generally called the M band [13]. Under light excitation in this spectral range, they show Stokes-shifted broad photoemission bands peaked at 678 nm and 541 nm [1], respectively, whose intensities can be detected by an optical microscope operating in fluorescence mode. Due to their high emission efficiencies [1] and lasing characteristics, even at RT, many investigations are reported in the literature about the spectral properties of these defects in LiF crystals and thin films coloured by several types of radiation.

High-contrast soft X-ray micro-radiographies of biological samples and metallic masks placed in close contact with LiF thin films were obtained at high spatial resolution by using brilliant laser-driven plasma sources operating under vacuum in the extreme ultraviolet (20 to 200 eV) and soft X-ray (200 eV to 2 keV) spectral ranges [3,4]. At these energies, their short attenuation length in LiF is of the order of 20-100 nm and 0.1-10 μm, respectively [14], and spatial resolution down to 80 nm in LiF films was demonstrated [15].

LiF film detectors about 1 μm thick allow for two-dimensional (2D) imaging with an X-ray tube operating at 8 keV, whose attenuation length of ~325 μm is much higher than the film thickness; a wide dynamic range, covering 3 orders of magnitude of dose up to 10^4 Gy, was demonstrated under laser excitation at 443 nm, although at the expense of the detection efficiency [7].

With hard X-rays from a synchrotron white beam up to 60 keV, in-line coherent diffraction imaging experiments were successfully performed for the first time [6] with reasonably short exposure times (1-30 s) in LiF crystals and thin films, only 1 μm thick. A linear relation of both the F_2 and F_3^+ emission intensities for doses from 10^4 to 10^6 Gy was experimentally found; such a linearity allows for a quantitative analysis of the fluorescence profiles and a careful comparison with simulations of theoretical X-ray intensity profiles of a coherent diffracted polychromatic beam.

In recent years, the use of hadrons in oncological radiotherapy has seen a remarkable growth because of the excellent ballistic properties of heavy particles, which lose their energy at the end of their path in tissue, called Bragg peak, with a modest lateral diffusion, thus preserving the surrounding healthy organs during tumour irradiation. For energies higher than 1 MeV, protons going through insulating materials lose their energy primarily by ionisation and excitation of atoms. Furthermore, tissue-equivalence of LiF material makes passive radiation detectors based on CC visible RPL very attractive for advanced proton beam diagnostics, even at clinical doses [11]. During the construction of a linear modular accelerator at ENEA C.R. Frascati for protontherapy applications [16], proton beams of nominal energy 3 and 7 MeV were used to irradiate LiF crystals and thin films in a wide dose range from 6×10^2 to 10^7 Gy. The proton irradiation induces the local formation of stable CCs, mainly the primary F centres and the aggregate F_2 and F_3^+ ones. Using a fluorescence microscope, the transversal proton beam intensity was mapped by acquiring the visible RPL images of the irradiated spots, thanks to the high emission efficiency of F_2 and F_3^+ defects. Despite of the film low thickness, 2D transversal dose maps were reconstructed at low proton energies [17], even at the highest doses, by introducing a simple model to describe the integrated RPL behaviour as a function of dose. Moreover, the high intrinsic spatial resolution and the wide dynamic range of the LiF radiation detectors allowed to obtain images of the whole Bragg curve [10] and their full reconstruction up to proton energy of 35 MeV, even at clinical doses in LiF crystals [11].

For a quantitative analysis of fluorescence profiles in radiation imaging as well as for dosimetry applications, the relationship between the F_2 and F_3^+ RPL signals and the irradiation time/dose should be investigated, depending on the form of LiF material.

In this work, some systematic results about the RPL dose-response of F_2 and F_3^+ defects in proton-irradiated polycrystalline LiF thin films, thermally-evaporated both on glass and reflective silicon substrates, are presented and discussed, in comparison with LiF crystals. Recent achievements in the enhancement of sensitivity for these LiF film radiation detectors grown on reflective substrates are

compared also with results obtained for X-ray irradiation, with the aim of highlighting the opportunities offered by their deposition technique [2,4,17].

2. Materials and Methods

The irradiated samples were commercially-available, surface-polished LiF single crystals of thickness 1 mm, and optically transparent polycrystalline LiF thin films, ~0.8 μm thick, thermally-evaporated on glass and Si(100) substrates kept at a constant temperature of 300 °C during the deposition process [18], which was performed in a vacuum chamber at a pressure below 1 mPa at ENEA C.R. Frascati. The starting material consisted of LiF microcrystalline powder (Merck Suprapur, 99.99% pure) that was heated at about 800 °C in a water-cooled tantalum crucible. The substrates were mounted on a rotating sample holder, which allows to accommodate several substrates in the same deposition run and to achieve good thickness uniformity. The deposition rate was controlled at 1 nm/s by an INFICON quartz oscillator.

Optical properties of the LiF films were studied by analysing direct transmittance and/or absolute specular reflectance spectra, depending on the substrate optical transparency, measured by using a Perkin-Elmer Lambda 900 spectrophotometer.

LiF crystals and thin films were exposed perpendicularly to proton beams of 3 and 7 MeV nominal energies produced by the linear accelerator for protontherapy under development at ENEA C.R. Frascati [16]. A 50 μm thick kapton window was placed at the output of the machine beamline, which reduced the impinging protons energy to 2.23 and 6.65 MeV, respectively. The average beam current was 1 μA in 60 μs-long pulses at a repetition frequency of 50 Hz. The irradiation fluence covered the range of 10^{11}-10^{15} p/cm^2 by varying the total number of pulses delivered to the LiF samples.

After exposure, the accumulated transversal proton spatial distributions were measured by acquiring the latent 2D fluorescence images stored in the LiF thin layers by a fluorescence microscope Nikon Eclipse 80-i C1, equipped with a filtered Hg lamp and an Andor Neo s-CMOS camera, with an 11-bit dynamic range.

The RPL spectra of proton-irradiated LiF crystals and films grown on glass were measured at RT by pumping in a continuous-wave regime with the 457.9 nm line of an Argon laser, which allows to simultaneously excite the green and red emissions of F_3^+ and F_2 CCs. The RPL signal was spectrally filtered with a monochromator and acquired by means of a photomultiplier with lock-in technique. The RPL spectra were corrected for the instrumental calibration.

PL-excitation (PLE) spectra were collected at RT with a Horiba Scientific Fluorolog-3 spectrofluorimeter Model FL3-11, equipped with a 450 W Xenon lamp and a Hamamatsu R928 photomultiplier, adopting a front-face detection geometry.

3. Results and Discussion

Figure 1(a) shows the direct transmittance and absolute specular reflectance spectra of a LiF film thermally-evaporated on a fused silica substrate, Suprasil®, measured between 190 and 1200 nm. The spectra of the bare substrate are also shown for comparison. The interference fringes, due to the refractive index differences between the LiF film and the substrate, are a signature of the film good optical quality, planarity and uniformity. By using a best-fit procedure with an analytical model [19], the complex refractive index and several physical features of the layer can be quantitatively estimated. It should be taken into account that the polycrystalline nature of LiF thin films could imply a reduced density of the LiF films, which can be considered as an aggregate of grains with air interstices. As a matter of fact, from the best fit procedure, a refractive index of (1.349 ± 0.002) at the wavelength of 633 nm was derived, which is lower than the bulk one (1.391); an extinction coefficient of (5.75 ± 1.72) × 10^{-4} and an average thickness of (854 ± 1) nm were obtained, together with a surface root mean-square roughness of (16.3 ± 0.2) nm. A deviation from parallelism of the film faces of (1.9 ± 0.3) % and a linear inhomogeneity along the growth axis of (-1.5 ± 0.4) % were also estimated.

According to Monte Carlo simulations performed with SRIM software [20], the linear energy transfer (LET), which is the linear density of energy deposited by protons, reported in Fig.1(b) for proton beams of 2.23 and 6.65 MeV impinging on bulk LiF of density $\rho = 2.635$ g/cm^3, continuously increases with depth, reaching the maximum value, the Bragg peak, almost at the end of the implantation path.

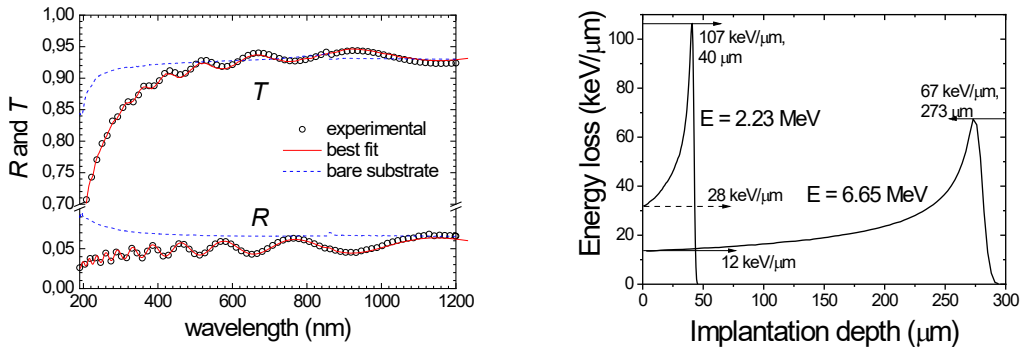

(a) (b)

Figure 1. (a) Direct transmittance and specular reflectance spectra of a LiF film, ~0.8 μm thick, thermally-evaporated on a fused silica substrate kept at a constant temperature of 300 °C during the deposition, and their best-fit, see the text for details. The measured spectra of the bare substrate are also shown for comparison. (b) SRIM simulation of LET for 2.23 and 6.65 MeV proton beams as a function of depth in a LiF crystal. The LET values at the air-LiF interface and at the Bragg peaks are reported, together with their depth position.

The initial LET value is higher at the lowest energy and raises to a maximum at the Bragg peak. At these low proton energies, the particle penetration in LiF is well below the LiF crystal dimensions, but it is much larger than the film thickness (~0.8 μm), thus the LET can be assumed to be constant within LiF films, with a very small fraction of the proton energy being deposited in them. On the contrary, in 1 mm thick LiF crystals, radiation induced defects are produced inside a volume whose depth is comparable with the implantation depth of impinging protons, within which they lose all their energy.

The integrated RPL intensities of the proton-irradiated spots in LiF crystals and thin films, carefully extracted from the fluorescence images exposed at different irradiation times for both proton energies, are reported in Fig.2(a) as functions of the average dose deposited in the irradiated LiF volume. The RPL experimental curves in Fig.2 are obtained from the same set of samples (LiF crystals and thin films) irradiated at both proton energies; in Fig.2a the spectrally integrated PL signal is measured by a fluorescence microscope on the entire proton-irradiated areas at both energies; the measurement errors can be estimated ±2%. In Fig.2b the distinct F_2 and F_3^+ contributions are derived from laser excited RPL spectra at the proton energy of 2.23 MeV. The measurement errors can be estimated ±6%, which may be influenced by the centering of the laser spot on the colored irradiated areas. It should be noted that, in both figures, the x-axis is the Volume-averaged dose, in Gy, which takes into account the differences between crystals and thin films in terms of thickness and dose-depth distribution. Due to the limited thickness, the volume-averaged dose coincides with the local value of dose only in LiF thin films.

A linear optical response was obtained over about three order of magnitude of doses, up to saturation dose values, after which PL quenching is observed. This behaviour can be described by using an elementary defect formation model [17] that takes into account the RPL intensity dependence

on the energy released in the material and the saturation of CC concentrations at high doses. The best fit of the integrated PL intensities I_{PL} can be obtained according to the following expression:

$$I_{PL} = A\left[1 - \exp\left(-\frac{D}{D_{sat}}\right)\right]$$

where D is the absorbed dose and D_{sat}, the saturation dose, is defined as the dose value above which saturation begins to be evident.

Due to the limited thickness of LiF films, the RPL intensity values are the same for the LiF films at both proton energies [9] in the whole investigated dose interval. It means that the concentrations of stable color centers created by ionization are proportional to the dose in the investigated proton energy range and they appear to be independent of the dose-rate between 12 and 28 keV/μm. In the case of thick LiF crystals, the RPL signal, which is proportional to total number of defects in the optically pumped coloured volume, is from ~30 to ~300 times greater in LiF crystals than in LiF films, depending on the irradiation energy, due to the deeper penetration of protons (see Fig.1(b)).

The best fit of the integrated RPL signal provided the values of the saturation doses [17], which result to be larger in LiF films with respect to crystals at both energies. The saturation doses were recognised to depend on several factors, among them the nature of the samples, i.e. single crystals [17,21] or polycrystalline thin films [9,22], the proton energies [9,21], but also the types of CCs [21,22] – all of them are relevant for quantitative proton beam diagnostics by LiF-based detectors.

Figure 2(b) shows the distinct F_2 and F_3^+ RPL vs. dose contributions at 2.23 MeV for LiF crystals and polycrystalline films, as derived from the laser-excited PL spectra. The F_2 and F_3^+ emission bands in the PL spectra of proton irradiated LiF films exhibited the same spectral features (peak positions and half-widths) of irradiated LiF crystals [22] and remained unchanged in the investigated dose range.

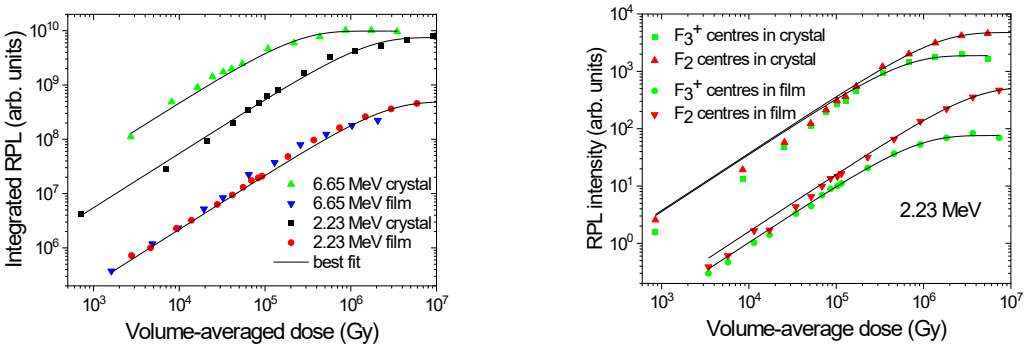

(a) (b)

Figure 2. (a) Integrated visible RPL signal as a function of the proton dose in LiF crystals and thin films grown on a glass substrate irradiated by 2.23 and 6.65 MeV proton beams, as derived from optical fluorescence images. The solid lines are the best fits, see the text for details. (b) F_2 and F_3^+ PL intensities vs. dose in LiF crystals and thin films grown on a glass substrate irradiated by 2.23 MeV proton beams, as derived from RPL spectra under continuous-wave laser excitation at 458 nm. The solid lines are their best fits according to the same model.

Again, a linear optical response as a function of the dose was obtained over about three order of magnitude, up to saturation, after which PL quenching started. From the best fit, distinct saturation values for F_2 and F_3^+ CCs were found in LiF crystals, $D_{sat} = (1.27 \pm 0.09) \times 10^6$ Gy for F_2 defects, greater than $D_{sat} = (5.25 \pm 0.54) \times 10^5$ Gy for F_3^+ ones [21].

For both kinds of defects, higher values were found in LiF films, $D_{sat} = (3.26 \pm 0.04) \times 10^6$ Gy for F_2 CCs and $D_{sat} = (7.29 \pm 0.54) \times 10^5$ Gy for F_3^+ ones. Such a difference could be explained by taking

into account that in the crystal the Bragg peak is located inside the optically excited volume: volume portions of irradiated crystals that are in the proximity of the Bragg peak, from which most of the RPL comes, absorb much more dose than the volume-averaged dose, and therefore their CCs concentration saturates apparently earlier than in a thin film. Radiation damage of LiF at high doses is quite complex and many theoretical and experimental works provide interesting results about the effects of ion irradiation at high doses, not only as far as the optical properties are concerned [23], but also when morphological and structural ones are considered [24], depending on particle mass and energy. However, the full understanding of the formation and stabilization processes of radiation-induced aggregate CCs, including colloids formation [25], and their effects on the RPL mechanisms is far to be predictable in LiF crystals; these investigations are still in their infancy in polycrystalline LiF films [26]. As a matter of fact, other experimental evidences, not reported here, suggest that we cannot exclude that formation and stabilisation processes involving aggregate CCs can be influenced by the polycrystalline nature of the films, which increases the maximum defects density due to the higher surface-to-volume ratio and reduces the formation of larger aggregate CCs at the grain boundaries.

By using optical reflective substrates, it is possible to increase the collection efficiency of the RPL signal emitted by CCs during the fluorescence reading process and, consequently, the sensitivity of the LiF film-based detectors. Figure 3(a) shows the integrated visible RPL intensities, carefully derived from the fluorescence images of the spots exposed at different doses for the proton-irradiated LiF films thermally evaporated on glass and those grown on Si(100) substrates in the same deposition run. For the coloured LiF films grown on Si, an increase of more than 50% of the RPL signal was measured with respect to the LiF films deposited on glass substrates (see Fig.3(a)). This enhancement is ascribed to both the F_2 and F_3^+ CCs spectral emission contributions [18], as confirmed by the PLE spectra measured at the peak wavelength of their PL bands. As example, in Fig.3(b), the PLE spectra at the emission wavelength of 678 nm, on the peak of F_2 emission, of two LiF films, grown on glass and Si(100) substrates and subsequently proton-irradiated at the same dose of 3.8×10^5 Gy, which is below the saturation threshold found in Fig.2(b), are compared. On the peak, the enhancement of the spectral contribution raises to 75% for the film grown on Si(100).

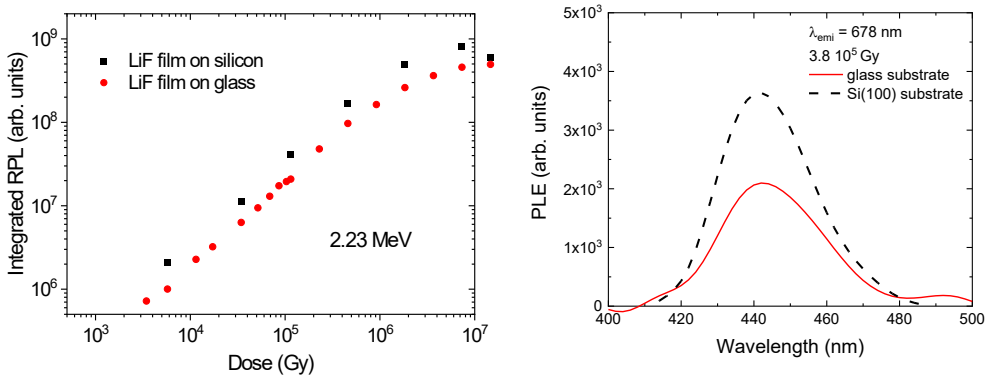

(a) (b)

Figure 3. (a) Integrated visible RPL intensity vs. dose in LiF thin films grown on glass and Si(100) substrates in the same deposition run, irradiated by 2.23 MeV proton beams, as derived from optical fluorescence images. (b) PLE spectra of two LiF films, grown on glass and Si(100) substrates, irradiated by 2.23 MeV proton beams at the same dose and measured at the emission wavelength of 678 nm.

Such an enhancement is due to a fraction of RPL that is recovered by reflection from the Si substrate and collected by the microscope detection system, while it gets lost through the substrate if

this latter is the glass one. A uniform distribution of CCs within a LiF film grown on a reflecting substrate, whose main purpose is to redirect the otherwise lost fraction of visible RPL towards the fluorescence microscope detection system is the most elementary example of light-confining structure. In the case of the broad visible emission of F_2 and F_3^+ CCs in a LiF film deposited on a Si substrate, it provides a sensible improvement of its performances as compared to a SiO_2 substrate.

For comparison, the RPL intensities coming from two LiF thin films, about 1 μm thick, grown in the same evaporation run on a glass and a Si substrate at 300 C, after single-shot soft X-ray irradiation with a laser-plasma source equipped with a Cu target developed at Tor Vergata University in Rome [27,28], were measured. During irradiation, identical metallic meshes were placed in contact with the LiF film surfaces. The fluorescence images stored in the LiF film detectors thermally evaporated on glass and Si substrates are shown in Figs.4(a) and (b), respectively, where the dark areas correspond to the nickel mesh wires, which are opaque to the incident X-rays. The fluorescence image in Fig.4(b) is brighter, due to the presence of the reflective substrate, as confirmed by the RPL intensity profiles measured along horizontal lines of the images, shown in Fig.4(c) for the coloured LiF films deposited on both substrates. The integrated RPL signal measured on the LiF film on Si is ~65% higher than the one collected from the LiF film on glass, a value which is comparable with those obtained in the proton-irradiated samples, as the entire film thickness should be coloured in this irradiation conditions.

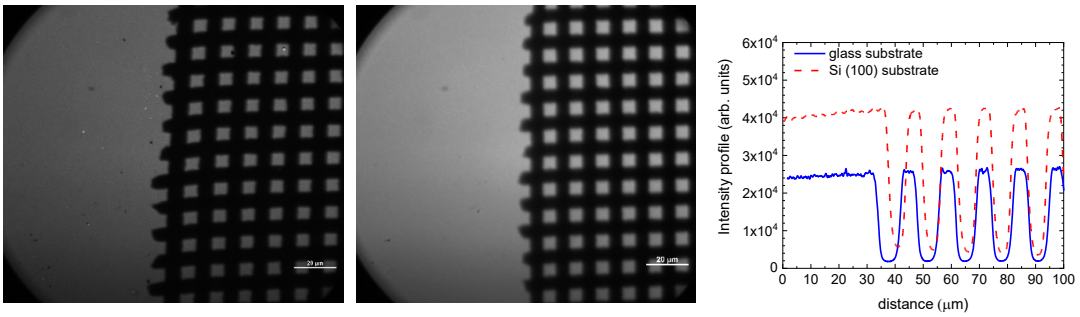

(a) (b) (c)

Figure 4. Fluorescence images of the top surface of LiF films, about 1 μm thick, grown on a (a) glass and (b) Si(100) substrate, after irradiation with soft X-rays. (c) PL intensity profiles acquired along horizontal lines obtained by image analysis.

4. Conclusions

The RPL signal intensities of aggregate F_2 and F_3^+ CCs in proton-irradiated LiF films are at least one order of magnitude lower than in LiF crystals irradiated at the same doses because only a small fraction of the total proton energy is released in its limited thickness, the rest being deposited in the substrate. This fact notwithstanding, optically transparent thin LiF film detectors are able to locally store information about the proton beam intensity with high sensitivity in a wide dynamic range. Despite of their low thickness, the linear behaviour of the integrated visible RPL intensities over at least three orders of magnitude of dose, makes them suitable for bi-dimensional solid-state dosimeters, even at high proton doses.

Their sensitivity at low doses can be increased by choosing suitable reflective substrates, which help to recover both the red and green broad emission of F_2 and F_3^+ CCs. This simple approach, based on the compatibility of thermally-evaporated LiF films with the Si(100) substrate, is in principle valid for any kind of ionising radiation, like X-ray photons, and increases the visibility of the latent florescence images stored in the detectors, although therapeutic dose values that are typical of clinical radiotherapy are still a big challenge.

All the reported results are very encouraging for advanced dose diagnostics of low-energy proton beams at high spatial resolution with LiF film detectors based on the visible RPL of radiation-induced aggregate CCs.

Acknowledgments
Research partially carried out within the TOP-IMPLART (Oncological Therapy with Protons - Intensity Modulated Proton Linear Accelerator for RadioTherapy) project, funded by Regione Lazio, Italy and the TECHEA (Technologies for Health) project. The authors are indebted with P. Gaudio, L. Picardi and C. Ronsivalle for skillful support and fruitful discussions.

References
[1] Basiev T T, Mirov S B, Osiko V V 1988 *IEEE J. Quantum Electron.* **24** 1052
[2] Montereali R M 2002 *Handbook of Thin Film Materials* vol 3, ed H S Nalwa (San Diego: Academic Press) chapter 7 pp 399-431
[3] Baldacchini G, Bonfigli F, Faenov A, Flora F, Montereali R M, Pace A, Pikuz T, Reale L 2003 *J. Nanoscience and Nanotechnology* **3**, 6 483
[4] Montereali R M, Bonfigli F, Piccinini M, Nichelatti E, Vincenti M A 2016 *J. Lumin.* **170** 761 and references therein
[5] Pikuz T A, Faenov A Y, Fukuda Y, Kando M, Bolton P, Mitrofanov A, Vinogradov A V, Nagasono M, Ohashi H, Yabashi M, Tono K, Senba Y, Togashi T, and Ishikawa T 2013 *Appl. Optics* **52**, 3 509
[6] Bonfigli F, Cecilia A, Heidari Bateni S, Nichelatti E, Pelliccia D, Somma F, Vagovic P, Vincenti M A, Baumbach T and Montereali R M 2013 *Rad. Meas.* **56** 277-280
[7] Kurobori T, Matoba A 2014 *Jpn. J. Appl. Phys.* **53** 02BD
[8] Villarreal-Barajas J E, Piccinini M, Vincenti M A, Bonfigli F, Khan R, Montereali R M 2015 *IOP Conf. Series: Materials Science and Engineering* **80** 12020 pp.1-5
[9] Piccinini M, Ambrosini F, Ampollini A, Picardi L, Ronsivalle C, Bonfigli F, Libera S, Nichelatti E, Vincenti M A and Montereali R M 2015 *Appl. Phys. Lett.* 106 261108
[10] Nichelatti E, Piccinini M, Ampollini A, Picardi L, Ronsivalle C, Bonfigli F, Vincenti M A and Montereali R M 2017 *Europhysics Letters* **120** 56003-1-5
[11] Piccinini M, Nichelatti E, Ampollini A, Bazzano G, De Angelis C, Della Monaca S, Nenzi P, Picardi L, Ronsivalle C, Surrenti V, Trinca E, Vadrucci M, Vincenti M A, Montereali R M 2020 *Rad. Meas.* **133** 106275_1-4
[12] Sekatskii S K, Letokhov V S 1996 *Appl. Phys. B* **63** 525
[13] Nahum J and Wiegand D A 1967 *Phys. Rev.* **154** 817
[14] http://henke.lbl.gov/optical_constants/atten2.html
[15] Ustione A, Cricenti A, Bonfigli F, Flora F, Lai A, Marolo T, Montereali R M, Baldacchini G, Faenov A, Pikuz T and Reale L 2006 *Jpn. J. Appl. Phys.* **45** 3B 2116
[16] Ronsivalle C et al. 2015 *Eur. Phys. Lett.* **111** 14002
[17] Piccinini M, Nichelatti E, Ampollini A, Picardi L, Ronsivalle C, Bonfigli F, Libera S, Vincenti M A and Montereali R M 2017 *Europhysics Letters* **117** 37004
[18] Leoncini M, Vincenti M A, Bonfigli F, Libera S, Nichelatti E, Piccinini M, Ampollini A, Picardi L, Ronsivalle C, Mancini A, Rufoloni A, Montereali R M, 2019 *Opt. Mat.* **88** 580
[19] Montecchi M, Montereali R M and Nichelatti E 2001 *Thin Solid Films* **396**, 264; 2002 *Thin Solid Films* **402**, 311
[20] Ziegler J F, Ziegler M D and Biersack J P 2010 *Nucl. Instrum. Meth. B* **268** 1818
[21] Nichelatti E, Piccinini M, Ampollini A, Picardi L, Ronsivalle C, Bonfigli F, Vincenti M A and Montereali R M 2019 Optical Materials **89** 414
[22] Montereali R M, Ampollini A, Picardi L, Ronsivalle C, Bonfigli F, Libera S, Nichelatti E, Piccinini M, Vincenti M A 2018 *J. Lum.* **200** 30

[23] Abu- Hassan L H and Townsend P D 1998 *J. Phys. C: Solid State Phys.* **19** 99
[24] Lushchik A, Lushchik Ch., Schwartz K., Vasil'chenko E., Papaleo R., Sorokin M., Volkov A. E., Neumann R., and Trautmann C. 2007 *Phys. Rev. B* 76 054114
[25] Seifert N, Liu D, Aldbridge R G, Barnes A V, Tolk N, Husinsky W and Betz G 1992 *Phys. Rev. B* **46** 1
[26] Kumar M, Singh F, Khan S A, Tripathi A, Avasthi D K, Pandey A C 2007, *J. Lumin.* **127** 302
[27] Montereali R M, Bonfigli F, Vincenti M A and Nichelatti E 2013 *Il Nuovo Cimento C* **36**, 2 35
[28] Richetta M, Francucci M, Gaudio P, Martellucci S, Bellecci C, Toscano D, Rydzy A, Gelfusa M, Ciuffa P 2006 *J. Phys. Condens. Matter* **18** 2039